COVID-19 detection using chest computed tomography scans on Ecuadorian patients who live in the highland region

Jacho Hernández, Kelding Jahemar y Martínez Moposita, Danny Mauricio

Departamento de Eléctrica Y Electrónica

Carrera de Ingeniería en Electrónica e Instrumentación

Artículo académico, previo a la obtención del título de Ingeniero en Electrónica e Instrumentación

Ing. Guerrón Paredes, Nancy Enriqueta, Ph.D.

Latacunga, 22 de noviembre del 2021

COVID-19 DETECTION USING CHEST COMPUTED TOMOGRAPHY SCANS ON ECUADORIAN PATIENTS WHO LIVE IN THE HIGHLAND REGION

This is the subtitle of the paper, this document both explains and embodies the submission format for authors using Word

KELDING JAHEMAR, K.J.J.-H., JACHO HERNANDEZ*

Departamento de Eléctica y Electrónica, Universidad de las Fuerzas Armadas ESPE, kjjacho@espe.edu.ec

DANNY MAURICIO, D.M.M.-M., MARTINEZ MOPOSITA

Departamento de Eléctica y Electrónica, Universidad de las Fuerzas Armadas ESPE, dmmartinez2@espe.edu.ec

NANCY ENRIQUETA, N.E.G.-P., GUERRON PAREDES

Departamento de Eléctica y Electrónica, Universidad de las Fuerzas Armadas ESPE, neguerron@espe.edu.ec

MAYRA JOHANNA, M.J.E.-R., ERAZO RODAS

Departamento de Eléctica y Electrónica, Universidad de las Fuerzas Armadas ESPE, mjerazo@espe.edu.ec

ABSTRACT

The early detection of COVID-19 is one of the current challenges in developing effective diagnosis and treatment mechanisms for patients who are at a high risk for community contagion. Computed Tomography (CT) is an essential support for detecting the infection pattern that causes this disease. CT scans provide relevant information on the morphological appearance of the infected parenchymal tissue, known as ground-glass opacities. Artificial Intelligence (AI) can assist in the quick evaluation of CT scans to differentiate COVID-19 findings in suggestive clinical cases. In this context, AI in the form of, Convolutional Neural Networks (CNN), has achieved successful results in the analysis and classification of medical images. A deep CNN architecture is proposed in this study to diagnose COVID-19 based on the classification of Chest Computed Tomography (CCT) images. In this study 8,624 CCTs of Ecuadorian patients affected by COVID-19 in the first quarter of 2021, were examined. The initial review of CCTs was performed by medical experts to discriminate the CCTs against other chronic lung diseases not associated with COVID-19. The CCTs were pre-processed by techniques such as morphological segmentation, erosion, dilation, and adjustment. After training the model reached an overall F1-score of 97%.

CCS CONCEPTS

•Applied computing; • Life and medical sciences; • Computational biology; • Imaging;

Additional Keywords and Phrases: Chest Computerized Tomography, Convolutional Neural Networks, COVID-19, Deep Learning, Lung Segmentation

ACM Reference Format:

First Author's Name, Initials, and Last Name, Second Author's Name, Initials, and Last Name, and Third Author's Name, Initials, and Last Name. 2018. The Title of the Paper: ACM Conference Proceedings Manuscript Submission Template: This is the subtitle of the paper, this document both explains and embodies the submission format for authors using Word. In Woodstock '18: ACM Symposium on Neural Gaze Detection, June 03–05, 2018, Woodstock, NY. ACM, New York, NY, USA, 10 pages. NOTE: This block will be automatically generated when manuscripts are processed after acceptance.

1 Introduction

SARS-CoV-2, commonly known as COVID-19, is a virus identified for the first time in the Province of Wuhan, China, during the last days of December 2019. This virus is characterized by symptoms such as fever, dry cough, generalized weakness, diarrhea, loss of taste or smell, respiratory distress, and chest pain or pressure [1]. The high rate of spread of COVID-19 caused the death of more than 4 million people, who developed severe pulmonary diseases [2]. In this context, the development of mechanisms for early identification of COVID-19 in the lungs is vital, since this could reduce the rate of spread of the disease [3]. The Reverse Transmission Polymerase Chain Reaction (RT-PCR) test is a fundamental tool for the diagnosis of COVID-19; however, further challenges persist such as high false negative rates, variability in testing techniques, and low sensitivity of 60-70% [4].

Chest Computed Tomography (CCT) is an essential diagnostic tool for the clinical management of COVID-19 associated with lung diseases, which allows early detection and timely treatment of patients[4], [5]. A prospective initial analysis conducted in Wuhan revealed that 40 of 41 CCTs of patients with COVID-19 showed similar patterns such as bilateral pulmonary opacities [6]. Another study examined the 22 CCTs of infected patients, all these cases showed ground-glass opacities and consolidation, occasionally with a rounded morphology and peripheral pulmonary distribution [7]. Normally, the identification of lung lesions in CCT is manual, however, the increasing number of suspected and confirmed cases of COVID-19 made a tedious and laborious work with highly variable diagnoses for the medical expert [8]. In this scenario, Machine Learning (ML) is a useful tool for automatic, fast and efficient detection of patterns suggestive of COVID-19 in CCT [9].

The scientific literature describes several ML methods applied to medical imaging processing, such as Support Vector Machines (SVM), Decision Tree-based Learning (DTL), Naive Bayes (NB), and Deep Learning (DL) [9], [10]. The DL algorithm is one of the most efficient techniques for these applications, because its accuracy rate is adequate for the diagnosis and prediction of various acute and chronic lung diseases. The development of Convolutional Neural Networks (CNN) algorithms has revealed promising results as the medical diagnoses provided by these tools compared favourably with the diagnoses given by experts [11]–[13].

This research aims to develop an AI model to predict ground-glass opacities and consolidations caused by COVID-19 in CCT slices. The collected data consists of 8,624 CCT slices from two kinds of images: COVID-19 and non-COVID-19. These CCT slices were pre-processed with segmentation techniques to get two different masks: lung and infection. The original CCT slices with their respective masks are the input data to train the proposed CNN. The results were analyzed using metrics such as precision, recall and binary classification F1-score.

This article is structured as follows: In section 1, Introduction. In section 2, Materials and Methods. In section 3, Results and Discussion. In section 4, Discussion. Finally, Conclusion is in section 5.

2 Materials and Methods

2.1 Data Acquisition

The data used in this work was collected from the Clinical and Pathological Laboratory “BioImagenes”, Ambato, Ecuador. The complete CCTs are uploaded daily to the private cloud "AMBRA HEALTH" in Digital Imaging and Communication on Medicine (DICOM) format, in this cloud the specialist can analyze each CCT in detail and determine medical reports. The authors signed a non-disclosure agreement of the data analyzed in this work.

The data used 8,460 CCTs, of which 7,723 CCTs were from confirmed COVID-19 patients, and the remainder were CCTs from healthy people. The data was initially examined in detail by medical specialists to diagnose COVID-19 in each patient. With this data, we created the CCT slices dataset (COVID-19 and non-COVID-19). Figure 1(a) shows the difference between the CCT slice of a patient with COVID-19 and, (b) a healthy patient. The presence of ground-glass opacities and consolidation with a peripheral distribution in bilateral lung areas can be seen in the infected lungs [14].

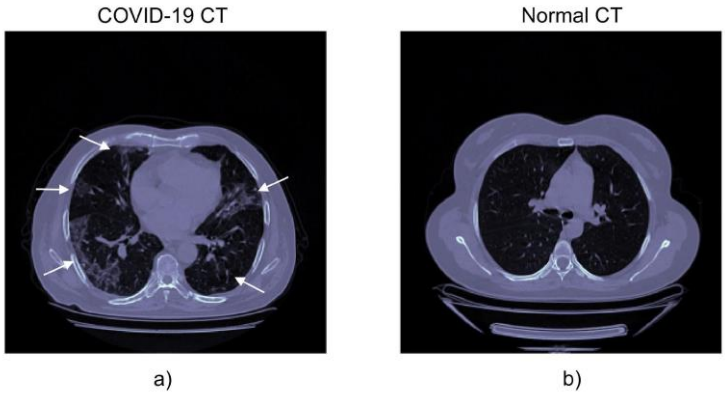

Figure 1. Patient CCT slices (a) COVID-19 confirmed. (b) Healthy.

2.2 Computational Resources

For the development of the proposed CNN, we used the following hardware specifications: CPU intel Core i7 2.20GHz (8750H) processor, RAM 16GB and GPU Nvidia GeForce GTX 1060 XGB dedicated memory. This was used to train, validate and test the proposed CNN, as well as data pre-processing and test in order to prove the computational efficiency of the proposed CNN.

In this case, we used the integrated development environment (IDE) Spyder for scientific programming Python version 3.9. Spyder integrates powerful libraries for the design of neural networks. The Keras software is a powerful, easy-to-use and free open-source Python library for developing and evaluating deep learning models. Furthermore, with Keras it is possible to export the CNN architecture and weights in an open-source format called HDF (Hierarchical Data Format) 5th version Pythonic (H5PY). The GPU environment is enabled in Spyder IDE, based on the technology Nvidia provided by the GPU, that allows parallel computing. In this way we speed up the proposed CNN.

2.3 Data pre-processing

The CCTs in (DICOM) format initially have a 512x512 pixel matrix that stores intensities in Hounsfield Units (HU). Figure 2 (a), show how the CCT slices provide information about the lung tissue, which allows the identification of potential abnormalities in the parenchymal tissue. An image segmentation process was performed on each CCT. The Lung Mask (LM) was obtained by separating the lungs with infected tissue from the rest of the body's tissues, with intensities of -300HU or higher. Likewise, the Segmented Lung Mask (SLM) was separated into intensities of -700HU or higher. In (c) the Binary fill was done to the SLM in order to solidify the lung morphology. Finally, the Infection Mask (IM) was obtained through the subtraction between LM and SLM. And also, in (b) the Erosion and dilation techniques were applied for better segmentation of the infected tissue (IM). The SLM was obtained to identify the focused area. The IM was obtained to distinguish the infection zones for easy detection.

The CCTs and their respective IM and SLM layers were saved in Neuroimaging Informatics Technology Initiative (NifTI) format, in order to obtain the CCT volume for each patient. At this point, each file has a matrix size (x,512,512), where x is the number of slices generated by one CCT. Then all the slices enter in a pre-training phase where they are resized to a size of (x,224,224).

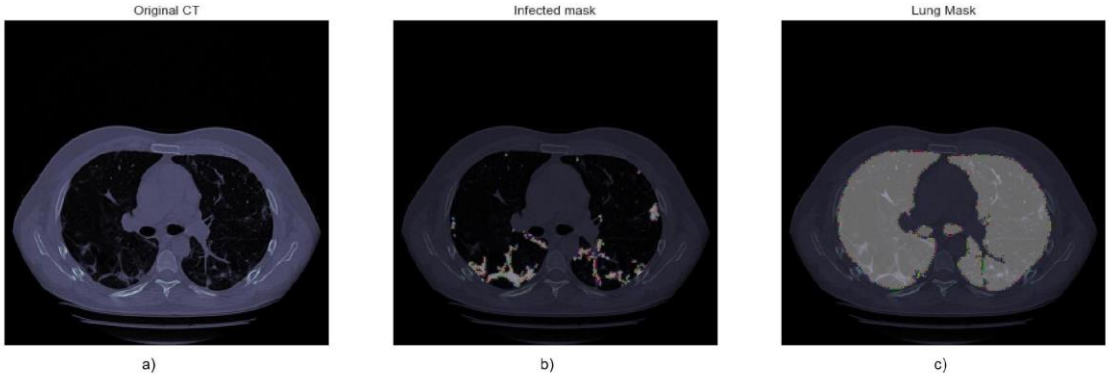

Figure 2. CCTs Pre-processing Technique. (a) A previously selected CT slice with COVID-19 disease. (b) The infection masks. (c) The segmented lung masks. Images (b) and (c) were obtained from the original CT slice (a).

2.4 Convolutional Neural Network (CNN)

CNNs are deep artificial neural networks that simulate the visual system of the human brain, and thus can be used in the fields of image recognition, analysis, and classification [15]. A CNN contains multiple convolutional layers of one or more dimensional, max-pooling, and nonlinear layers. CNN's convolutional layer is recognized as the main one, and it is responsible for the feature extraction phase of the image. The main layer kernel is applied to the layer inputs, and then all the layer outputs are convolved to obtain a feature map. The convolution operation is nonlinear using equation 1,so the CNN needs to adapt to a nonlinear function. In this study, the Rectified Linear Unit (ReLU) was used as an activation function in each convolutional layer, in order to increase the nonlinearity in the input image due to the images being mainly non-linear.

The convolution layer is responsible for taking the neighboring pixel groups from the input image, performing the scalar product with a kernel that goes through the entire input image from left to right and from top to bottom, generating a new output matrix, which is turned into a new layer of hidden neurons. In this project, 16, 32 and 64 filters were used for the required convolutional layers. In each filter phase, hidden layers, also called feature maps, are obtained from the original large-size image, which needs high time processing. A subsampling layer was implemented to minimize the over-fitting in the feature extraction, decreasing the size of the feature map and returning the relevant features detected by each filter. Artificial data augmentation was used to avoid over-fitting, this is used when there are a limited number of CCT volumes. This study used image rotations, horizontal and vertical rotations and cropping techniques. The feature pooling can be between the maximum, average, and sum of the CNN model. Max-pooling is applied to identify the essential features detected by the previous layer. The dropout layer was also utilized with a 40% dropout rate [16]. In the last CNN stage, a flattening layer was implemented, which converts the three-dimensional output of the convolutional layers into a vector with one-dimensional features. The flattening layer organizes the characteristic data outputs obtained by the convolutional layers into a vector. Once the flattening is completed, the vector data becomes an input for the next layer, which is called the fully connected layer. In the fully connected layer, each neuron in the flattened layer is directly connected to each correspondent neuron for a binary classification. By doing so, the CNN network with the fully connected layer decides the classification probability.

$$x_n = \sum_{k=0}^{N-1} y_k f_{n-k} \tag{1}$$

For N number of elements and f filter, where y is the signal. The output vector is represented by x

2.4.1 *The proposed CNN Architecture.*

The architecture of the proposed CNN model consists of 6 convolution layers, 6 max-pooling layers, 6 dropout layers, 6 activation functions layers, 6 batch normalization layers, 1 flatten layer, and 2 dense layers (see Figure 3). The dimension of the input image of the CNN model is 224x224. Furthermore, for each convolution layer (Conv2D), these are convolved with their respective kernel of size 3x3and with 1 stride, later filters of sizes 16, 32, and 64 were used respectively. After each convolution layer, the batch normalization layer was used to normalize the output activations, and then it applied the max-pooling layer to the feature map. Also, ReLU activation function is deployed. The dropout rate is 40% in the dropout layer. Finally, the last convolution layer produces a 3D matrix, which enters a flatten layer to be converted into a vector that will be the input for 2 dense layers.

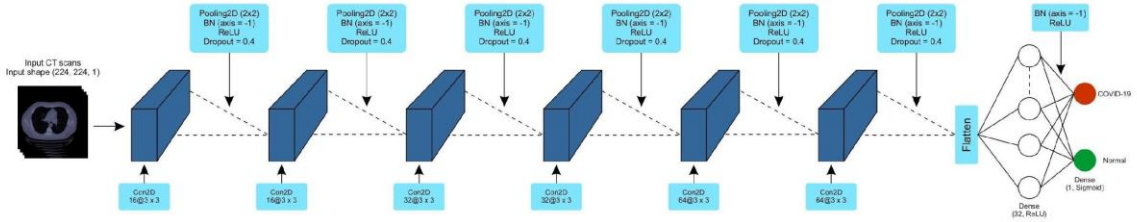

Figure 3. The Proposed CNN architecture.

This study used a CNN model for binary classification, so it applied the binary cross-entropy (BCE) loss function [17]. The binary classification only needs one output node to classify the data into one of the two given classes: COVID-19 and non-COVID-19. A sigmoid activation function is assigned to the BCE in order to reduce its size. The sigmoid activation function has a value between 0 and 1. This allows finding the error between the predicted class and the real class. The BCE loss function is defined in equation 2 and is used in the last layer of the proposed CNN model. CNN experiments were initially performed with different configurations, with respect to the number number of convolutional layers in the model. The number of convolutional layers implemented was chosen using an incremental learning approach, without compromising the model accuracy [18]. At first, it was implemented a CNN with 4 convolutional layers; then the results of the 5-layer convolutional CNN architecture were analyzed. The approach continued up to results obtained by the model exceeded 95% for metrics: accuracy and F1-score. The final model consists of 6 convolutional layers and the model results were analyzed in the results section.

$$L = -\frac{1}{N}\left[\sum_{i=1}^{N}[t_i * log\,(p_i) + (1-t_i) * log\,(1-p_i)]\right] \quad (2)$$

For N data points, where t_i is the truth value taking a value of 0 or 1, p_i is the softmax probability for ith data.

2.5 Model Training and Testing

This proposed model was trained for 25 epochs. The "Adam" optimizer was used to improve precision and to reduce the loss of the learning model. The trained network was stored in H5PY format so that it can be used at any time. The trained network took each patient's pre-processed CCT volume and COVID-19 probability results (positive as well as negative). The predicted probabilities of all patients with their corresponding truth labels were studied for statistical analysis.

2.6 COVID-19 statistical analysis

COVID-19 detection results were analyzed using the accuracy and the F1 score given by the training model. The F1 score is the harmonic average of precision and recall (Equation 4). Also, “Precision” is the fraction of all positive predictions that are true positives (Equation 2). Continuing this, “Recall” is the fraction of all true positives that are predicted as positive (Equation 3). And in the end, the maximum value that the F1 score can reach is 1 [19].

$$Precision = \frac{TP}{TP + FP} \quad (2)$$

$$Recall = \frac{TP}{TP + FN} \quad (3)$$

$$F1 = 2 * \frac{Precision * Recall}{Precision + Recall} \quad (4)$$

Where TP is the true positive, FP is the false positive, and FN is the false negative.

3 RESULTS AND DISCUSSION

In this study, the F1-score was used to classify patients with COVID-19 against patients in normal conditions. Table 1shows that the obtained results, with an F1-score of 97% and 95% for patients with COVID-19 and healthy lungs, respectively. The precision and recall results are also shown. The results were validated by a medical specialist.

Table 1. Performance results for CNN model metrics, COVID-19 vs. non-COVID-19.

Class	Precision	Recall	F1-score
COVID-19	97%	98%	97%
Non COVID-19	95%	95%	95%
Accuracy	96%		

A total of 4,800 CCTs were used to validate the system. Figure 4shows 4 examples of the model results. In sections (a) and (b), the algorithm detected ground-glass opacities caused by COVID-19. On the other hand, in sections(c) and (d), the algorithm did not detect any abnormal patterns in the lungs and classified them as healthy patients.

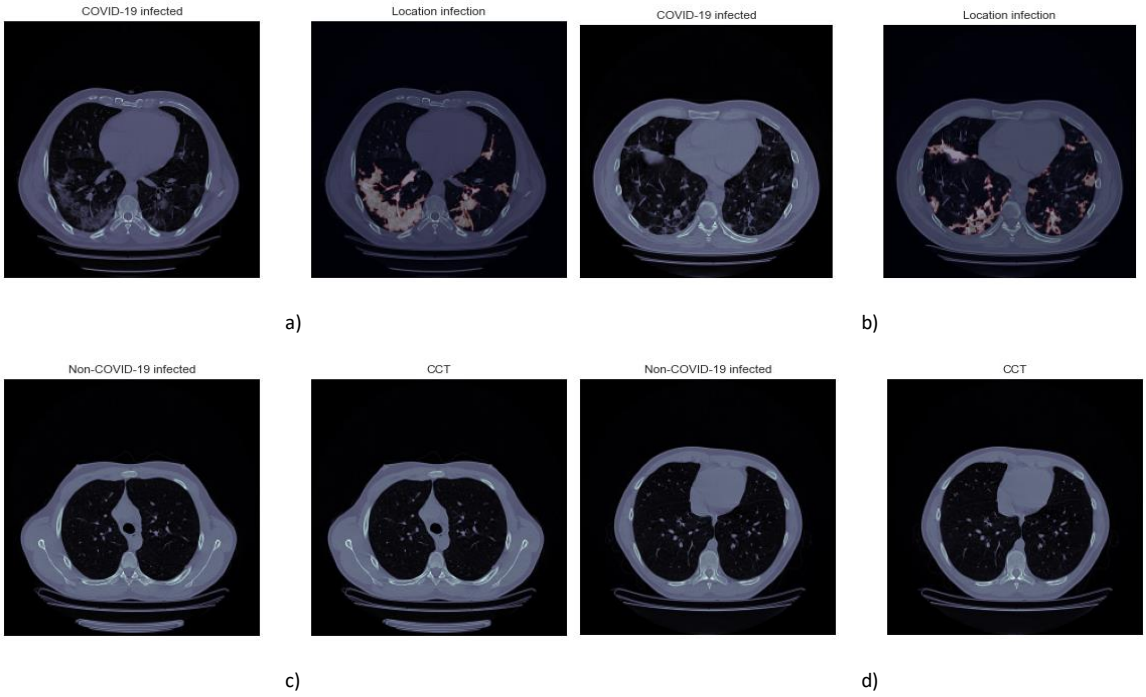

Figure 4. The predicted results of 4 different patients: Sections (a) and (b) correspond to two CT scans (left) and their location infection (right) of COVID-19 patients. Sections (c) and (d) correspond to two CT scans (left) and the repeated image without infect.

As mentioned in the section 2.4.1, the model was built on an incremental learning approach. Starting with a 4-layer convolutional architecture, an increment of a convolutional layer was performed in each experiment and the results were analyzed. Table 2 illustrates the precision metric and F1-score results after each increment from 4 convolutional layers to a stable model consisting of six convolutional layers. The comparison of the incremental learning approach is shown in Figure 5.

Table 2. Accuracy and F1-score with different number of CNN Layers.

Convolutional layer	Accuracy (%)	F1-score (%)
Four Conv2D	89%	88%
Five Conv2D	92%	93%
Six Conv2D	97%	97%

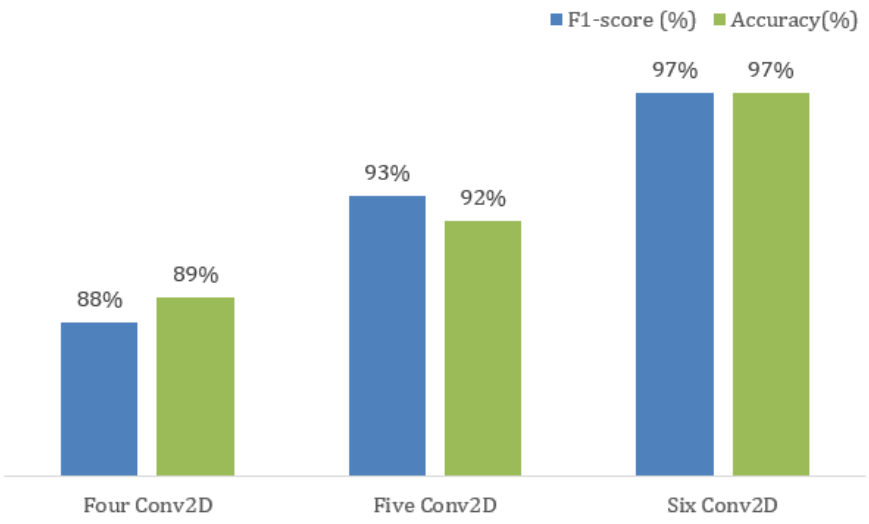

Figure 5. Accuracy and F1-score with different number of CNN Layers.

The main advantage of the proposed model relays on its methodology for obtaining the aforementioned masks. All these masks were created for the model, so it can focus to learn about the lung's work area (SLM), and also on detecting infected tissue by IM. The mask files generated in section 2.2 are compatible with several medical image analysis tools such as FMRIB Software Library (FSL) and ITK-SNAP [20] that can be read, written and manipulated by engineering software such as Java and Matlab. On the other hand, in the pre-training phase, CCTs are sliced using the lung mask and resized to a size (224x224). This proposed methodology is different from the models described in [21], [22]. In the first model [21] does not implement any pre-processing methodology, while the second model [22] obtains the wavelet coefficients from each CCTs as inputs to the network.

With regard the performance parameter metrics obtained with the proposed model in this study, we reached the highest accuracy compared to models [21] and [22]. As shown in Table 3, Author [21] obtained the lowest accuracy. The values of precision and recall reached by the author [22], were in the middle of [21] and our model. [22]. In addition, the accuracy and F1 score of the proposed model contrast with the same kind of values of the author [22]. Overall, this suggested method achieves better results than other cutting-edge techniques.

Table 3. Comparison of the results of the proposed model with previous models.

Studies	Pre-processing	Accuracy (%)	Precision (%)	Recall (%)	F1-score (%)
Polsinelli [21]	NO	85.03	85.01	87.42	86.20
Matsuyama [22]	YES	92.2	92.2	90.81	91.5
The Proposed CNN	YES	96.53	97.55	94.93	96.18

4 Conclusion

In this study, some image segmentation techniques have been executed in DICOM format, which were transformed into NIfTI format for the input of the CNN model slices, from which two kinds of masks were obtained: At first, a pulmonary mask which used the binary fill for the whole lung tissue's masking. Meanwhile, a second mask, the infection mask, worked with the morphologic techniques of dilatation and erosion that stand up the unnatural tissue.

The experimental analysis of the CNN, viewing a pulmonic resizing and segmentation in the images, confirms the good results given by this kind of models for the identification of the characteristic patterns of COVID-19 inside the lungs.

The algorithm developed in this research achieved a remarkable performance in the detection of COVID-19 patterns, inside the CCT process, increasing the efficiency of the diagnostic precision of COVID-19 consequences, which makes the job easier for medical specialists.

ACKNOWLEDGMENTS

We are grateful for the collaboration of the Clinical and Pathological Laboratory "BioImágenes" for supplying us with the images used in this study and the technicians who verified the classified images.

REFERENCES

[1] G. P. Inca Ruiz and A. C. Inca León, "Evolución de la enfermedad por coronavirus (COVID-19) en Ecuador," *La Cienc. al Serv. la Salud y la Nutr.*, vol. 11, no. 1, pp. 5–15, 2020, doi: 10.47244/cssn.Vol11.Iss1.441.

[2] Woldometer, "Covid-19 Coronavirus Pandemic," *Coronavirus Cases*. p. 1, 2020, [Online]. Available: https://www.worldometers.info/coronavirus/#countries.

[3] P. Pokhrel, C. Hu, and H. Mao, "Detecting the Coronavirus (COVID-19)," *ACS Sensors*, vol. 5, no. 8, pp. 2283–2296, 2020, doi: 10.1021/acssensors.0c01153.

[4] S. A. Harmon *et al.*, "Artificial intelligence for the detection of COVID-19 pneumonia on chest CT using multinational datasets," *Nat. Commun.*, vol. 11, no. 1, p. 4080, 2020, doi: 10.1038/s41467-020-17971-2.

[5] C. Jin *et al.*, "Development and evaluation of an artificial intelligence system for COVID-19 diagnosis," *Nat. Commun.*, vol. 11, no. 1, p. 5088, 2020, doi: 10.1038/s41467-020-18685-1.

[6] C. Huang *et al.*, "Clinical features of patients infected with 2019 novel coronavirus in Wuhan, China," *Lancet*, vol. 395, no. 10223, pp. 497–506, 2020, doi: https://doi.org/10.1016/S0140-6736(20)30183-5.

[7] M. Chung *et al.*, "CT Imaging Features of 2019 Novel Coronavirus (2019-nCoV)," *Radiology*, vol. 295, no. 1, pp. 202–207, 2020, doi: 10.1148/radiol.2020200230.

[8] Q. Yan *et al.*, "COVID-19 Chest CT Image Segmentation -- A Deep Convolutional Neural Network Solution," 2020, [Online]. Available: http://arxiv.org/abs/2004.10987.

[9] P. gifani, A. Shalbaf, and M. Vafaeezadeh, "Automated detection of COVID-19 using ensemble of transfer learning with deep convolutional neural network based on CT scans," *Int. J. Comput. Assist. Radiol. Surg.*, vol. 16, no. 1, pp. 115–123, 2021, doi: 10.1007/s11548-020-02286-w.

[10] B. J. Erickson, P. Korfiatis, Z. Akkus, and T. L. Kline, "Machine Learning for Medical Imaging," *RadioGraphics*, vol. 37, no. 2, pp. 505–515, 2017, doi: 10.1148/rg.2017160130.

[11] V. Shah, R. Keniya, A. Shridharani, M. Punjabi, J. Shah, and N. Mehendale, "Diagnosis of COVID-19 using CT scan images and deep learning techniques," *Emerg. Radiol.*, 2021, doi: 10.1007/s10140-020-01886-y.

[12] T. Goel, R. Murugan, S. Mirjalili, and D. K. Chakrabartty, "OptCoNet: an optimized convolutional neural network for an automatic diagnosis of COVID-19," *Appl. Intell.*, vol. 51, no. 3, pp. 1351–1366, 2021, doi: 10.1007/s10489-020-01904-z.

[13] S. S. Yadav and S. M. Jadhav, "Deep convolutional neural network based medical image classification for disease diagnosis," *J. Big Data*, vol. 6, no. 1, p. 113, 2019, doi: 10.1186/s40537-019-0276-2.

[14] F. Fu *et al.*, "Chest computed tomography findings of coronavirus disease 2019 (COVID-19) pneumonia," *Eur. Radiol.*, vol. 30, no. 10, pp. 5489–5498, 2020, doi: 10.1007/s00330-020-06920-8.

[15] C. Zheng *et al.*, "Deep Learning-based Detection for COVID-19 from Chest CT using Weak Label," *medRxiv*, p. 2020.03.12.20027185, Jan. 2020, doi: 10.1101/2020.03.12.20027185.

[16] A. A. Reshi *et al.*, "An Efficient CNN Model for COVID-19 Disease Detection Based on X-Ray Image Classification," *Complexity*, vol. 2021, p. 6621607, 2021, doi: 10.1155/2021/6621607.

[17] U. Ruby and V. Yendapalli, "Binary cross entropy with deep learning technique for image classification," *Int. J. Adv. Trends Comput. Sci. Eng.*, vol. 9, no. 10, 2020.

[18] A. Gepperth and B. Hammer, "Incremental learning algorithms and applications," 2016, [Online]. Available: https://hal.archives-ouvertes.fr/hal-01418129.

[19] Z. C. Lipton, C. Elkan, and B. Narayanaswamy, "Thresholding classifiers to maximize f1 score," *ArXiv*, pp. 1402–1892, 2014.

[20] "Segmentación activa del contorno {3D} guiada por el usuario de Estructuras anatómicas: eficiencia y confiabilidad significativamente mejoradas," *Neuroimage*.

[21] M. Polsinelli, L. Cinque, and G. Placidi, "A light CNN for detecting COVID-19 from CT scans of the chest," *Pattern Recognit. Lett.*, vol. 140, pp. 95–100, 2020, doi: https://doi.org/10.1016/j.patrec.2020.10.001.

[22] E. Matsuyama, "A Deep Learning Interpretable Model for Novel Coronavirus Disease (COVID-19) Screening with Chest CT Images," *J. Biomed. Sci. Eng.*, vol. 13, no. 07, pp. 140–152, 2020, doi: 10.4236/jbise.2020.137014.

Authors' Information

Your Name	Title*	Research Field	Personal website
Kelding Jahemar Jacho Hernández	Student	NA	https://orcid.org/0000-0001-5420-324X
Danny Mauricio Martínez Moposita	Student	NA	https://orcid.org/0000-0002-6992-8494
Nancy Enriqueta Guerrón Paredes	PhD	Biomedical	https://orcid.org/0000-0003-1971-4647
Mayra Erazo-Rodas	PhD	Telecommunication	https://orcid.org/0000-0002-2196-3514

***This form helps us to understand your paper better, and the form itself will not be published.**

***Title can be chosen from: Master Student, PhD Candidate, Doctor, Assistant Professor, Lecturer, Senior Lecturer, Associate Professor, Full Professor, Researcher, Senior Researcher**